Electric Power Systems Research 122 (2015) 42–49

Contents lists available at ScienceDirect

Electric Power Systems Research

journal homepage: www.elsevier.com/locate/epsr

Directional overcurrent relay coordination considering non-standardized time curves

Carlos A. Castillo Salazar[a,*], Arturo Conde Enríquez[a], Satu Elisa Schaeffer[a,b]

[a] Universidad Autónoma de Nuevo León, UANL, FIME, Ciudad Universitaria, San Nicolás de los Garza C.P. 66451, NL, Mexico
[b] Coordinación de Cómputo Científico, CIIDIT, UANL, PIIT Monterrey, Apocada C.P. 66600, NL, Mexico

ARTICLE INFO

Article history:
Received 14 August 2014
Received in revised form
19 December 2014
Accepted 20 December 2014

Keywords:
Directional overcurrent relay coordination
Non-standardized curves
Evolutionary computation
Genetic algorithms
Two fault levels
Multi-objective function

ABSTRACT

In this work, a directional overcurrent relay coordination is carried out considering more than one level of short-circuit current and non-standardized inverse time curves. A genetic algorithm is proposed and shown capable of obtaining adequate protection settings in a reasonable time. The algorithm designs a specific time curve for each relay, improving the results of the coordination process without compromising the compatibility of the curves.

1. Introduction

The *overcurrent relay* (OCR) is the simplest and cheapest among all protection principles. Despite the increased use of more sophisticated protections, it is still commonly used as primary protection on distribution and subtransmission systems and as a secondary protection on transmission systems for phase faults [1]. Although a three-phase short circuit occurs in less than 5% of cases, it is common for a conventional coordination process, among the ones reported in the literature, to only consider this fault magnitude. In 1996, taking into account the computational capacity at the time and seeking to avoid possible curve crossings, the IEEE established a standard set of curve shapes [2].

Existing literature seeks to facilitate achieving coordination; [1,3] employ a linear optimization model in order to solve the problem while one or two variables are considered as adjustable settings. The main issue in the approach is the requirement of a good initial guess and also the high probability of being trapped in local minima. Later, coordination problems have been approached with evolutionary algorithms. *Genetic algorithms* (GA) are proven to perform well while solving the coordination problem considering one and two adjustable settings; almost two decades ago [4] solved the coordination problem by implementing a GA. In similar works and dates [5,6] use respectively one and two adjustable settings and a GA to solve miscoordination problems; likewise [7] seek to reduce the tripping times of the overcurrent relays by using a continuous genetic algorithm. Later, [8,9] propose hybrid approaches to determine the optima for two adjustable settings. Furthermore [10] consider different levels of voltage to determine the optimal settings of overcurrent and earth fault relays. [11] propose the use of another adjustable setting; their genetic algorithm has the capability of selecting the best characteristic among a group of curves from different standards.

The above proposals considered standardized time curves while searching for the optimal settings of the *time dial setting* (dial), the *pickup current* (I_{pickup}), or the characteristic constants, combining optimization methods such as linear optimization and genetic algorithms. The cited contributions were aimed to ensure relay coordination for maximum faults – which are the most important. Nevertheless, those algorithms do not monitor whether the coordination is achieved for lower currents.

[12,13] propose different methods to avoiding curves intersections, i.e., to achieve the coordination for lower currents. The former consists of a trial-and-error curve fitting method that selects optimal values of the three parameters aforementioned; on the other hand, the latter inspects and eliminates curve intersections by modifying the dial and the multiple of the pickup current ($M = I_{sc}/I_{\text{pickup}}$) until coordination is achieved for currents lower than the

* Corresponding author.
E-mail addresses: carlos.castillosl@uanl.edu.mx (C.A. Castillo Salazar), con_de@yahoo.com (A. Conde Enríquez), elisa.schaeffer@uanl.edu.mx (S.E. Schaeffer).

http://dx.doi.org/10.1016/j.epsr.2014.12.018
0378-7796/

Table 1
IEEE curve constants.

Curve type	*A*	*B*	*p*
Extremely inverse (EI)	28.2	0.1267	2
Very inverse (VI)	19.61	0.4910	2
Moderately inverse (MI)	0.0515	0.1140	0.02

maximum. Finally, [14] propose two algorithms that consider two magnitudes of short-circuit current (I_{sc}) in order to achieve the coordination. The sums of the tripping times of the main relays for the *close-in* and the *far-end* faults magnitudes are computed in order to evaluate the objective function of the proposed algorithms.

The use of curves with the same inversion grade does not always prevent curve crossings unless additional curve fitting is employed [12,13]; in addition, the tripping times of both main and backup relays tend to be high for those currents.

In this work we consider the tripping times of lower currents as well as the use of non-standardized inverse time curves to improve the coordination for the mentioned current levels. We carry out the coordination of overcurrent relays considering two different levels of I_{sc} and non-standardized inverse time curves, obtained by employing five parameters as adjustable settings. Presently, some commercial relays[1] – through software tools – already allow the user to define the curve parameters instead of simply selecting among the standardized ones.

2. Overcurrent protection

The goal of the *overcurrent relay coordination problem* consists of adjusting settings that drive a given protection system to optimal behavior, i.e., to minimize the relay tripping times as well as to ensure the coordination between main and backup relays for certain fault conditions [15,16]. In order to ensure the worst-case coordination, the OCR coordination is carried out using maximum fault currents and maximum or even critical demand conditions. The difficulty of setting up the relays and achieving coordination increases rapidly as the system grows, particularly in interconnected mesh power systems (IMPS).

A set of three shapes of inverse time curves are established in the IEEE standard C37.112-1996 [2]; the *moderately inverse* (MI), *very inverse* (VI), and *extremely inverse* (EI) curves are obtained by evaluating Eq. (1) for different levels of I_{sc}, using their respective constants illustrated in Table 1:

$$t = \left[\frac{A}{[I_{sc}/I_{pickup}]^p - 1} + B\right] \times \text{dial}, \tag{1}$$

where, t = time delay, I_{sc} = fault current, I_{pickup} = pickup current, dial = time dial setting, and A, B, p = characteristic constants.

The constants A, B, and p determine the inversion grade of the curve – limiting the shape of the curve may produce elevated or even unacceptable tripping times. With modern technology, a digital OCR could calculate an inverse time curve from given parameters in real time and even recalculate when required, instead of resorting to a predefined group of shapes.

In addition to dial and pickup current, the parameters A, B, and p can be considered as adjustable settings. Doing so provides more flexibility in the shape of the curves and consequently may facilitate relay coordination as well as reduce tripping times for maximum and minimum faults. This is applicable especially for highly interconnected power systems, where – due to the different magnitudes of load current (I_{load}) – the use of standardized curves cannot guarantee avoiding curve crossings.

[1] Siemens Reyrolle Protection Devices http://w3.siemens.com/smartgrid/global/en/products-systems-solutions/protection/reyrolle/pages/overview.aspx.

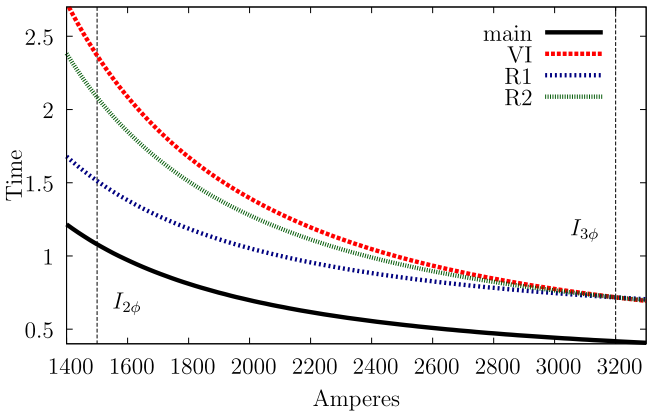

Fig. 1. Non-standardized inverse time curves compared with a conventional VI curve (as backups for a VI main protection shown with a continuous line).

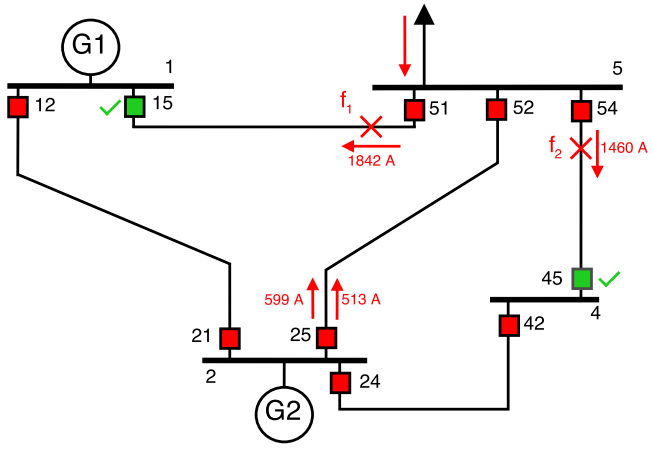

Fig. 2. Two faults simulated on a section of the IEEE 14-bus system [22].

Fig. 1 shows the inverse time curve for a single main relay which uses a VI curve and three possible backups for it: one is a standardized VI curve and the other two are non-standardized inverse time curves obtained with A, B, and p as adjustable parameters. Although the shapes of the curves do not differ remarkably, but the time reduction for the minimum current is notable.

2.1. Overcurrent relay coordination problem

Overcurrent relay has relative selectivity, meaning that it can be used as primary protection for the main line and as backup protection for an adjacent line. On radial systems, the current seen by the coordination pair is virtually the same; however, in an IMPS or one with distributed generation, the current seen by the main relay is higher than the one seen by the backup. In an example illustrated in Fig. 2, for a fault f_1 the main relay will see 1842 A while the relay 25 will only see 599 A. As can be noted, the relay 25 will have to operate as backup for the relays 51 and 54, increasing the complexity of coordination.

As can be seen in Fig. 2, the fault magnitude of each coordination pair is calculated independently and assuming that the opposite relay trips correctly, i.e., computing the short-circuit current of a close-in solid fault located immediately after the main relay with an open end. This procedure is carried out to simulate both two and three-phase faults. For the load currents, we consider the I_{load} of each relay in accordance with the load flow of its line [16].

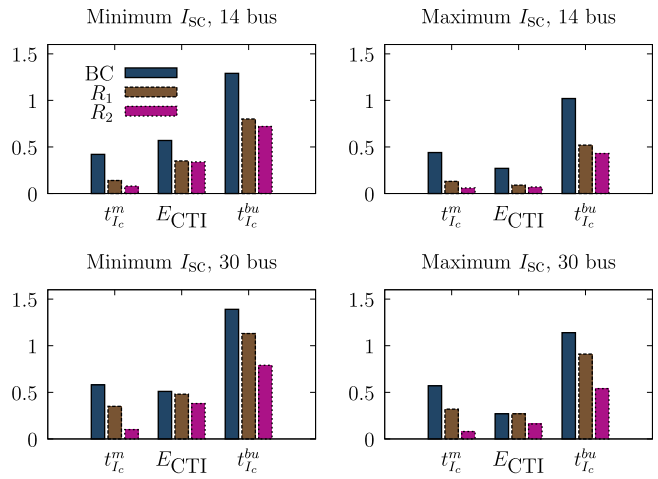

Fig. 3. The two sets of parameter ranges compared with a base case; each is evaluated for both maximum and minimum I_{sc}.

Coordination of a pair of relays is achieved when the tripping time of the backup protection is equal to the one of the main relay (t_m) plus a coordination time interval (CTI); the desired tripping time of the backup (t^d_b) is computed as

$$t^d_b = t_m + \text{CTI}. \quad (2)$$

In IMPS where a main relay commonly has more than one backup, an optimization method capable of performing such coordination is desirable. The performance of the method is increasingly important when multiple adjustable settings are considered.

2.2. Genetic algorithms

The choice of an algorithm capable to deal with problem constraints becomes a key factor in achieving optimal system performance, that is, increasing sensibility and reducing tripping times of the relays. As noted above, some optimization methods have previously been applied to the OCR coordination problem. In particular genetic algorithms provide a powerful technique of iterative searching and optimization, based on natural selection [17–19]. Even though some works (e.g. [20,21]) are exploring different methods capable to solve the coordination problem, adapting this technique to the OCR coordination problem is simple and functional, as discussed in existing literature [8,9,4,10,11].

Table 2
Parameter selection ranges.

Parameter	Minimum	Maximum
Dial	0.5	5
I_{pickup}	$1.4 \times I_{load}$	$2 \times I_{load}$
First set of ranges		
A	0.0515	28.2
B	0	0.4910
p	0.01	2
Second set of ranges		
A	0.01	50
B	0	1.5
p	0.01	5

3. Implementation of a GA for the OCR coordination problem

In this section, the proposed GA for the OCR coordination problem is described. Eq. (1) comprises six parameters, five of which are relay settings (dial, I_{pickup}, A, B, and p), the last one is the I_{sc}. In this work, the first five parameters are considered as adjustable settings, obtaining non-standardized inverse time curves.

3.1. Parameter ranges

A single range is considered for dial and I_{pickup} that are both directly proportional to the relay tripping time; consequently, higher values will lead the relay to an unwanted slowdown. Based on initial exploration of the effects of each parameter, we define two sets of ranges for the parameters A, B, and p, as specified in Table 2. The first set of ranges uses as lower and upper bounds the minimum and maximum values for each parameter from Table 1. The second set of ranges is wider in order to explore magnitudes outside the standard. Wider ranges result in a larger search space and therefore higher computation time.

3.2. Initial population

We refer to a candidate parameter configuration for the entire system as a chromosome. The set of chromosomes simultaneously considered by the algorithm at a given moment is called a population and the number of chromosomes in the population is denoted by TC. Initially, each parameter is assigned a value from the defined range of that parameter independently, uniformly at random. Increasing TC evidently increases the computational effort and consequently the simulation time, while improvements in the tripping times of main and backup relays are can be achieved. In our

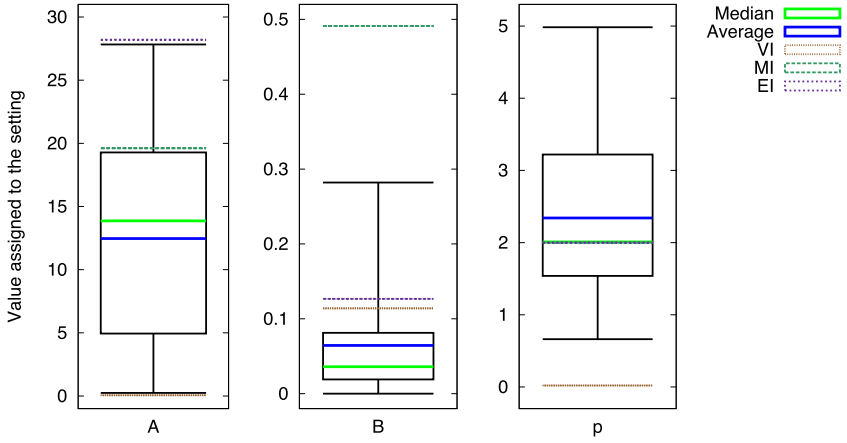

Fig. 4. Box-whiskers plots showing a comparison between computed settings and the standardized ones.

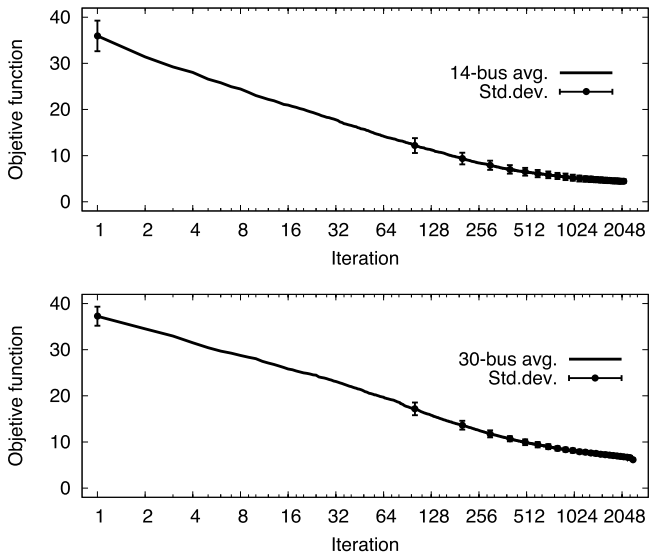

Fig. 5. Convergence of the genetic algorithm for the 14-bus and 30-bus systems.

exploratory experiments, using TC > 200 did not result in a reduction of miscoordinations while the improvements in tripping times were not substantial (cf. Fig. 7). Hence, we use TC = 200.

3.3. Objective function

The evaluation of the fitness of a chromosome consists of calculating the tripping time for main and backup relays, for both levels of I_{sc}: the desired time for each backup relay t_b^d of Eq. (2) would ideally be equal to the time achieved by the chromosome being evaluated (t_b^o). When the achieved time differs from the desired, the error of coordination time interval (E_{CTI}) is calculated as

$$E_{CTI} = t_b^o - t_b^d. \tag{3}$$

A pair of relays with a negative E_{CTI} is considered as a miscoordination. The number of pairs with negative errors is the total number of miscoordinations T_{mc}.

The main objective of this work is to achieve the coordination for a majority of protections while reducing tripping times for a maximum fault; our secondary objective is to achieve the same for a two-phase fault. Hence, our objective function consists of three parts – the first of them considers the total number of miscoordinations, the remaining two seek to minimize the tripping time of main and backup relays:

$$f(x) = \left\{ T_{mc} \times \alpha + \left(\sum_{i=1}^{TR} t_{m(i)} \right) \times \beta + \left(\sum_{j=1}^{TP} t_{b(j)} \right) \times \gamma \right\}, \tag{4}$$

where TR denotes the number of relays, TP the total number of coordination pairs, and $t_{m(i)}$ and $t_{b(j)}$ are the tripping times of main relay i and backup relay j, respectively, allowing a main relay to have more than one backup; finally α, β, and γ are weighting factors (we use constants in [0, 1]) that determine the importance of each factor, depending on the system requirements, that play an important role in the final results, as illustrated by our experiments. Even though the units are not consistent (the number of miscoordinations is combined with seconds), each of the three aspects is a desired characteristic (this is a common practice in multi-criteria optimization, combining aspects such as time and cost in one objective function). It can be noted that E_{CTI} is not explicitly present in the objective function, but rather has an implicit effect: it is used to calculate the number of miscoordinations and it is also used to penalize the backup times of the miscoordinated relays, multiplying each of these times by a fixed penalty factor ξ (we use $\xi = 10$ in our experiments) previous to the evaluation of the objective function, using the penalized times in the above summations.

As we seek the reduction of tripping times for currents lower than the three-phase current, we combine two evaluations of the above objective function of Eq. (4), once for the three-phase fault and again – with a smaller weight defined by a constant δ – for a two-phase fault, and use the sum of the two as the fitness of a given chromosome:

$$f_T(x) = f_{3\phi}(x) + \delta \times f_{2\phi}(x). \tag{5}$$

3.4. Selection and genetic operations

From the chromosomes of a given population, the population of the following generation is created by selecting parent chromosomes to create new chromosomes.

First, in order to guarantee that the next generation is not worse than the present one, the first 5% of the next-generation population is formed by including as such the highest–fitness chromosomes of the present generation (without considering duplicates). Secondly, in each iteration, a fraction of the entire population of the previous generation is subjected to a mutation. The percentage of the population subjected to mutations depends on whether the maximum fitness of each generation has improved over the past generations: when 50 generations pass without improvement in the best fitness within the population, 40% of the population are mutated to drastically increase diversity, whereas other generations are subjected to 5% mutations.

The remainder of the next generation is created by reproduction, carried out as a simple one-point crossover between two parent chromosomes. The crossover point is established uniformly at random between 25% and 75% of the total relays. We employ roulette-wheel selection, using the fitness of each chromosome to determine the probability of its selection as a parent, permitting

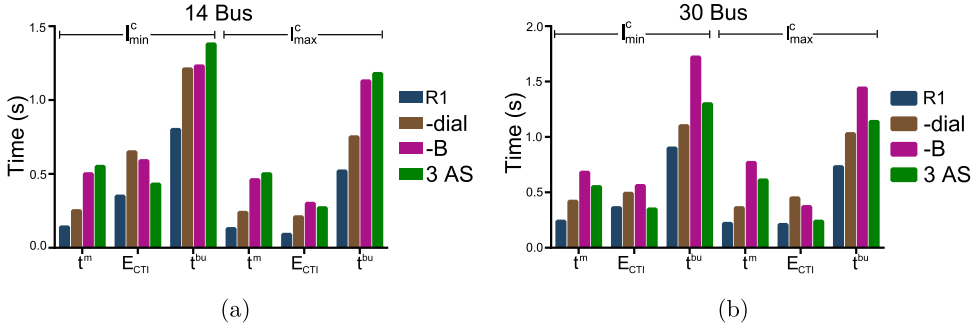

Fig. 6. Tripping times and errors considering five, four, and three adjustable settings. (a) 14-bus system. (b) 30-bus system.

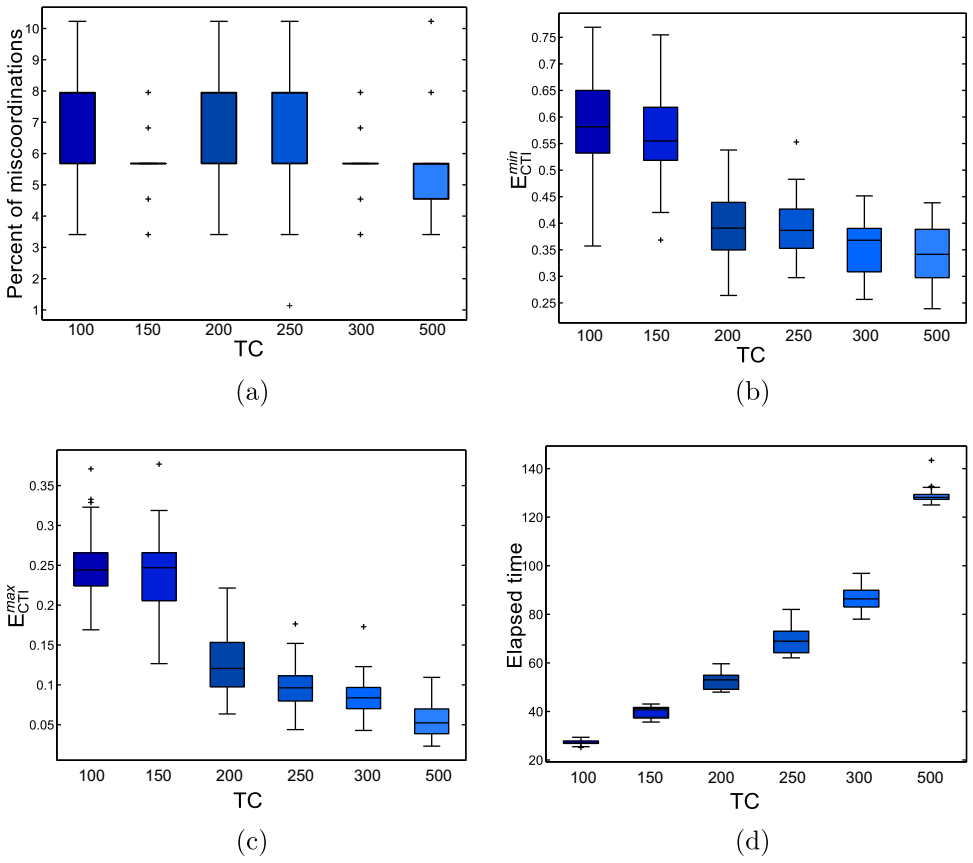

Fig. 7. Box-whiskers plots showing a comparison of measurements for different values of TC. (a) Percent of miscoordinations vs. TC. (b) $E_{CTI}^{2\phi}$ (s) vs. TC. (c) $E_{CTI}^{3\phi}$ (s) vs. TC. (d) Elapsed time (s) vs. TC.

multiple selection of each chromosome. No chromosome is directly discarded; even the worst one could be selected, although with low probability, thus permitting a higher diversity within the population and helping to avoid premature convergence to local minima.

4. Results

The two sets of parameters ranges were tested on the IEEE 14 and 30-bus systems [22]; the diagrams of the systems are shown in Fig. 8a and b, respectively. In addition to the two ranges, a base case (BC) was computed varying only the dial and the pickup current. Following common practice [15,16], the BC only uses VI (thus fixing the values of A, B, and p), curves and a constant δ equal to zero; namely, the minimum short-circuit current is not considered. For the two sets of ranges and the base case, we assume that the directional function of the relays operates correctly and is adjusted with the maximum sensitivity angle.

Excluding all relays where $I_{sc^{2\phi|3\phi}} < 1.5 \times I_{pickup}$ (i.e., sensitivity filter), the 14-bus system has 44 coordination pairs, whereas the 30-bus system has a total of 115 coordination pairs. The load currents of both systems can be seen in Table in Appendix A. In both systems, each pair is coordinated for a maximum (3ϕ) and minimum (2ϕ) fault current. The presented results seek to assure the coordination of a phase protection, however, in a similar way, the methodology could be applied to a ground scheme.

We explored the possible values of weighting parameters of the objective function; a simple comparison on the 14-bus system for a small subset of possible assignments is shown in Table 3. Only the tripping times for a maximum I_{sc} are shown, but the behavior was similar for other magnitudes. Note that the first set of parameters is not fully dominated for any of the others; therefore it was selected for the rest of the experiments. We set α, β, and γ to 1, 0.1 and, 0.1, respectively. A similar methodology was used to determine the value of the δ parameter, fixing it at $\delta = 0.3$ for the remainder of the experiments.

Table 3
Objective function weighting parameters.

α	1	1	0	0	1	0.5	1
β	0.1	0	1	0	1	0.1	0.1
γ	0.1	0	0	1	1	0.1	0.5
T_{mc}	5	3	70	67	19	7	5
$t_m^{I_{3\phi}}$	0.13	2.57	0.02	0.01	0.10	0.18	0.14
$t_b^{I_{3\phi}}$	0.52	4.37	0.38	1.88	0.47	0.58	0.58

The constant α has a greater weighing in order to ensure the coordination of the majority of the pairs; similarly, the value for δ was chosen to emphasize coordination for a maximum short-circuit current. By modifying these weights one can improve certain desired features whilst worsen others, similar to the behavior of a Pareto front.

Table 4 shows the results of the mean time of all coordinated pairs, illustrated in Fig. 3. Furthermore, the total of miscoordinations (T_{mc}) and the mean E_{CTI} are shown. The percentage of reduction that each parameter achieved for each case in comparison with the base case is also shown. The data indicates that the introduction of additional adjustable settings improves the coordination of overcurrent relays of both systems (the base case has two, whereas both sets of ranges vary five variables). The second,

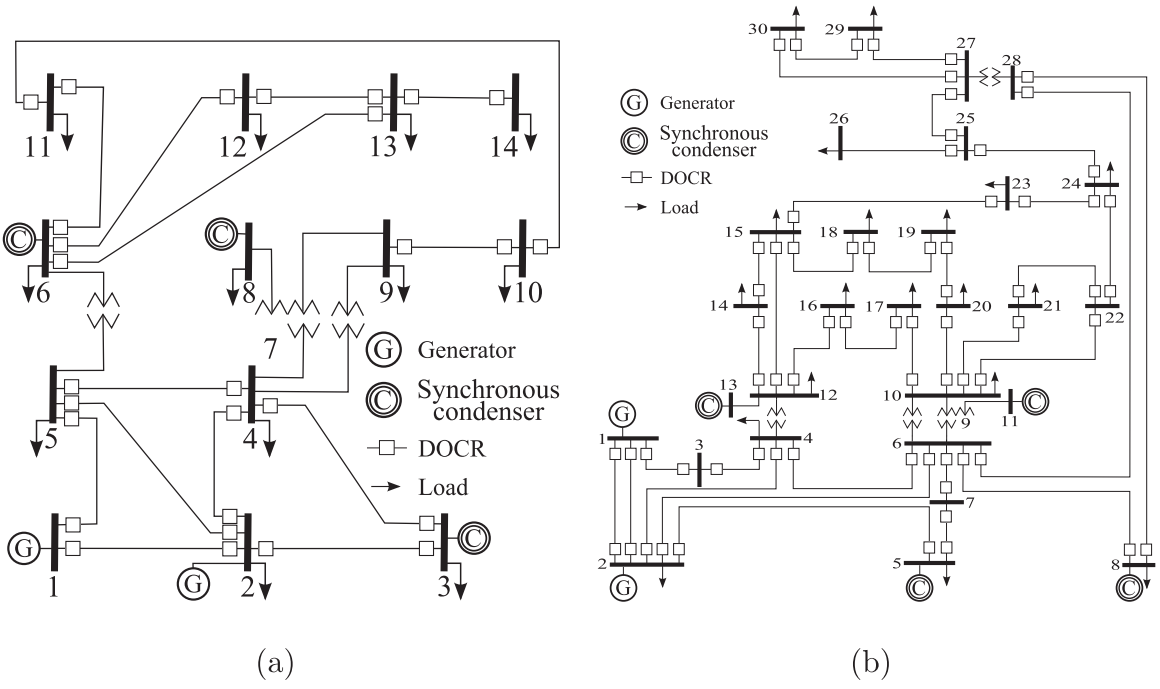

Fig. 8. Test systems. (a) IEEE 14-bus system. (b) IEEE 30-bus system.

Table 4
Mean times in seconds of all coordinated relays for the two sets of ranges (R1 & R2), compared with a base case (BC), with the respective reduction percentage (%).

Measure	BC	R1	%	R2	%	
14-Bus system						
T_{mc}	7	5	28.57	2	71.43	
t_m^{Ic}	0.42	0.14	66.24	0.08	81.46	
E_{CTI}	0.57	0.35	38.00	0.34	40.40	$I_c^{2\phi}$
t_b^{Ic}	1.29	0.80	38.43	0.72	44.47	
t_m^{Ic}	0.44	0.13	70.27	0.06	86.12	
E_{CTI}	0.27	0.09	68.54	0.07	73.52	$I_c^{3\phi}$
t_b^{Ic}	1.02	0.52	49.05	0.43	57.29	
Measure	BC	R1	% R	R2	% R	
30-Bus system						
T_{mc}	27	21	22.22	14	48.15	
t_m^{Ic}	0.58	0.35	40.53	0.10	81.99	
E_{CTI}	0.51	0.48	5.19	0.38	24.37	$I_c^{2\phi}$
t_b^{Ic}	1.39	1.13	18.88	0.79	43.25	
t_m^{Ic}	0.57	0.32	44.14	0.08	86.78	
E_{CTI}	0.27	0.27	2.20	0.16	40.86	$I_c^{3\phi}$
t_b^{Ic}	1.14	0.91	20.75	0.54	53.00	

wider range produces a higher number of coordinations[2]. For both short-circuit magnitudes, the mean tripping times of main and backups relays are reduced considerably in comparison with the base case.

Table 5 illustrates the settings and coordination errors for a single simulation of the 14-bus system [22], assuming that the transformers have their own protections. The relay identifications are conformed by the bus of origin and the bus of destiny of the line where each relay is placed, respectively. As expected, each relay has to operate as main and as backup protection with the same settings. The first column shows the main relays and the corresponding settings are shown on the following five columns. The following nine columns are divided in groups of three, as in this system each main relay has a maximum of three backups; each group represents a backup for the main relay of the corresponding row. For each coordination pair, the coordination errors for minimum and maximum fault are shown. The backup relays marked with an "S" on their E_{CTI} display a lack of sensitivity, while the ones with negative values did not coordinate. The settings (A, B, and p) that determine the shape of the resulting inverse time curves are compared to the standard-provided values in Fig. 4.

The convergence of the objective function (average and standard deviation over 30 simulations) is shown in Fig. 5 for the first range of parameter selection. In each iteration, a new generation is constructed as explained in Section 3. The values of the objective function in the figure are normalized in order to obtain comparable results between both systems: a value close to zero indicates the coordination of all pairs with very low tripping times. We use as a stopping condition a persistent lack of improvement in the objective function; note that the presence of a few miscoordinations is typical in real-world scenarios.

We studied the effect of the number of adjustable settings, comparing the results with those of the first set of parameter ranges (R1). Fig. 6 shows the results for three additional cases: in the first two (denoted by $-$dial and $-B$), the parameters dial and B were assigned fixed values (one and zero, respectively). A third alternative (denoted by 3 AS) permits the adjustment of dial, I_{pickup}, and chooses among the three IEEE standardized curves (Table 1), instead of freely adjusting A, B, and p. It is noteworthy that R1 achieves the lowest tripping times in all cases, thus outperforming the three alternatives with less adjustable settings. We had to widen the ranges of the adjustable settings in these three restricted cases to those shown in Table 6 in order to obtain a similar amount of miscoordinations between these new scenarios and R1. Also, the total of number of iterations increased for the new scenarios by 50%.

[2] We leave to future work the application of even broader parameter ranges that may lead to drastically different inverse time curves (potentially useful for industrial applications); in this work we chose to maintain shapes similar to the standardized ones.

Table 5
Settings and coordination errors for a single simulation of the 14-bus system.

Relay ID	Dial	Pickup multiplier	A	B	p	Backup ID	$I^{2\phi}$	$I^{3\phi}$	Backup ID	$I^{2\phi}$	$I^{3\phi}$	Backup ID	$I^{2\phi}$	$I^{3\phi}$
							E_{CTI}							
1-2	2.989	1.444	23.687	0.133	4.961	5-1	S	S	0	–	–	0	–	–
2-1	1.287	1.690	2.199	0.282	3.698	3-2	0.136	0.079	4-2	S	S	5-2	S	S
1-5	2.037	1.753	1.785	0.004	2.242	2-1	0.184	0.092	0	–	–	0	–	–
5-1	0.666	1.951	14.067	0.019	2.605	2-5	0.701	0.351	4-5	0.233	0.117	0	–	–
2-3	3.553	1.672	17.459	0.035	4.873	1-2	0.419	0.100	4-2	S	S	5-2	1.055	0.854
3-2	1.829	1.867	2.781	0.079	3.575	4-3	0.595	0.065	0	–	–	0	–	–
2-4	3.229	1.639	1.574	0.038	1.611	1-2	0.318	0.070	3-2	1.089	0.057	5-2	0.688	0.157
4-2	4.406	1.653	1.796	0.022	3.622	3-4	0.379	0.202	5-4	0.257	0.022	0	–	–
2-5	1.863	1.996	4.479	0.019	1.601	1-2	0.376	0.145	3-2	1.097	0.145	4-2	0.789	0.018
5-2	0.517	1.629	8.445	0.037	1.732	1-5	0.388	0.022	4-5	0.170	0.033	0	–	–
3-4	1.125	1.828	23.527	0.016	1.686	2-3	0.842	0.040	0	–	–	0	–	–
4-3	4.018	1.692	16.580	0.020	2.468	2-4	0.358	0.171	5-4	0.239	0.048	0	–	–
4-5	1.004	1.682	15.118	0.059	2.071	2-4	0.153	0.004	3-4	0.168	0.053	0	–	–
5-4	0.849	1.833	21.682	0.066	2.151	1-5	0.849	0.145	2-5	0.587	0.367	0	–	–
6-11	1.161	1.401	12.362	0.004	1.029	12-6	S	S	13-6	0.517	0.004	0	–	–
11-6	1.287	1.601	19.289	0.034	2.234	10-11	0.050	0.021	0	–	–	0	–	–
6-12	1.228	1.790	4.803	0.028	0.662	11-6	0.442	0.131	13-6	−1.199	0.177	0	–	–
12-6	0.562	1.402	5.371	0.000	4.984	13-12	0.039	0.010	0	–	–	0	–	–
6-13	1.246	1.408	19.248	0.004	1.203	11-6	0.195	0.013	12-6	S	S	0	–	–
13-6	0.874	1.519	0.240	0.182	1.414	12-13	0.075	0.073	14-13	0.102	0.023	0	–	–
9-10	0.560	1.556	27.827	0.004	3.890	14-9	0.173	0.026	0	–	–	0	–	–
10-9	2.921	1.473	5.774	0.114	1.517	11-10	−0.803	−0.770	0	–	–	0	–	–
9-14	1.707	1.888	24.077	0.082	1.787	10-9	0.053	0.016	0	–	–	0	–	–
14-9	1.113	1.660	20.347	0.030	2.151	13-14	0.235	0.126	0	–	–	0	–	–
10-11	1.312	1.639	13.657	0.151	1.264	9-10	−0.620	−0.599	0	–	–	0	–	–
11-10	0.510	1.420	15.914	0.002	3.425	6-11	0.098	0.041	0	–	–	0	–	–
12-13	3.196	1.830	7.291	0.166	1.948	6-12	0.112	0.014	0	–	–	0	–	–
13-12	1.630	1.554	8.296	0.078	0.957	6-13	0.179	0.070	14-13	0.1574	0.0588	0	–	–
13-14	2.280	1.982	19.836	0.055	1.634	6-13	0.240	0.128	12-13	0.0514	0.0622	0	–	–
14-13	0.625	1.589	14.143	0.170	1.239	9-14	0.171	0.031	0	–	–	0	–	–

Table 6
Parameter selection ranges for the comparison between different numbers of adjustable settings.

Parameter	Minimum	Maximum
I_{pickup}	$1.4\times I_{load}$	$3\times I_{load}$
A	0.01	50
p	0.01	5
For the case -dial		
B	0	5
	For the case $-B$	
Dial	0.5	10
	For the case 3AS	
Dial	0.5	10
B	0	5

5. Conclusions

In this work we demonstrate that the introduction of additional adjustable settings to the characteristic equation of inverse time curve improves the coordination between overcurrent relays, reducing the tripping times for the main and the backup protection for maximum and minimum fault currents. The total number of miscoordinations is reduced with the use of non-standardized time curves, while the curve shapes remain similar to the standardized ones. These observations permit us to conclude that the use of non-standardized time curves does not compromise the compatibility, but offers more flexibility.

Allowing for wider ranges for the adjustable settings lead to achieve better results, but seem to increase the computational load. Increasing the number of adjustable settings (we experimented with three, four, and five) also leads to better results.

Even though the addition of adjustable settings turns the basic coordination problem in a more complex one, this produces no burden to the user as the proposed algorithm performs the necessary adjustments. The sole requirement is the use of a commercial digital relay that allows for non-standardized time curves – some manufacturers already provide this option. The ranges of the adjustable settings and the weighting factors of the objective functions can be modified to give more importance to specific characteristics.

As future work, we consider the adaptation of diverse optimization methods other than genetic algorithms to ensure coordination of the overcurrent relays for a whole interval between minimum and maximum fault currents instead of the mere end points. Also, the effects of widening further the ranges of the adjustable settings is left to future work. Additionally, the coordination of those pairs are not considered due to their lack of sensitivity, another protection principle to achieve the coordination for those pairs needs to be incorporated into the algorithm.

Acknowledgments

The first author thanks CONACyT for a Ph.D. scholarship. The first author was visiting Aalto University and the third author was visiting researcher at HIIT at University of Helsinki during the final stages of the preparation of this work.

Appendix A. Further results

For the 14-bus system, 30 simulations were performed considering the first range of parameter selection, and values of TC $\in \{100, 150, 200, 250, 300, 500\}$. The results are shown in Fig. 7 as a set of box-whiskers diagrams where, for different values of TC, the percent of miscoordinations, the E_{CTI} for minimum and maximum fault currents, and the elapsed time of the simulations are plotted against the TC. Even though the use of more chromosomes improves the coordination process, the total number of miscoordinations remains practically the same. An increase in TC improves the tripping times, but also increases the computational effort

Table 7
Line loads for the simulated IEEE systems.

14-Bus system						30-Bus system					
Line	I_{line}	Line	I_{line}	Line	I_{line}	Line	I_{line}	Line	I_{line}	Line	I_{line}
1-2	624	3-4	99	9-10	27	1-2	720	12-14	136	21-22	39
1-5	298	4-5	260	9-14	40	1-3	362	12-15	317	15-23	98
2-3	294	6-11	32	10-11	16	2-4	185	12-16	132	22-24	110
2-4	224	6-12	32	12-13	7	3-4	353	14-15	29	23-24	37
2-5	167	6-13	73	13-14	24	2-5	346	16-17	66	24-25	40
						2-6	253	15-18	105	25-26	73
						4-6	320	18-19	48	25-27	82
						5-7	87	19-20	124	27-29	110
						6-7	166	10-20	163	27-30	125
						6-8	133	10-17	116	29-30	65
						6-28	83	10-21	313		
						8-28	17	10-22	149		

required. We set TC = 200 to allow the algorithm to obtain adequate protection settings in reasonable time.

The line loads of the 14-bus and 30-bus systems are shown in Table 7. The 14-bus and 30-bus systems diagrams are shown in Fig. 8a and b.

References

[1] A.J. Urdaneta, H. Restrepo, L.G. Pérez, Optimal coordination of directional overcurrent relays considering dynamic changes in the network topology, IEEE Trans. Power Deliv. 12 (4) (1997) 1458–1464.

[2] IEEE, IEEE Standard Inverse–Time Characteristic Equations for Over-current Relays, IEEE Std C37.112-1996, 1997, pp. 1–13.

[3] A.J. Urdaneta, H. Restrepo, L.G. Pérez, Optimal coordination of directional overcurrent relays in interconnected power systems, IEEE Trans. Power Deliv. 3 (3) (1988) 903–911.

[4] C. So, K.K. Li, K.T. Lai, K.Y. Fung, Application of Genetic Algorithm for Overcurrent Relay Coordination, in: Sixth International Conference on Developments in Power System Protection 6, 1997, pp. 66–69.

[5] F. Razavi, H.A. Abyaneha, M. Al-Dabbagh, R. Mohammadia, H. Torkaman, A new comprehensive genetic algorithm method for optimal overcurrent relays coordination, Electr. Power Syst. Res. 78 (2008) 713–720.

[6] A. Koochaki, M.R. Asadi, H.A. Abyaneh, R.A. Naghizadeh, M. Mahmoodan, Optimal Overcurrent Relays Coordination using Genetic Algorithm, in: 11th International Conference on Optimization of Electrical and Electronic Equipment, 2008, pp. 197–202.

[7] P.P. Bedekar, S.R. Bhide, Optimum coordination of overcurrent relay timing using continuous genetic algorithm, Expert Syst. Appl. 38 (2011) 11286–11292.

[8] P.P. Bedekar, S.R. Bhide, Optimum coordination of directional overcurrent relays using the hybrid GA-NLP approach, IEEE Trans. Power Deliv. 26 (1) (2011) 109–119.

[9] A.S. Noghabi, J. Sadeh, H.R. Mashhadi, Considering different network topologies in optimal overcurrent relay coordination using a hybrid GA, IEEE Trans. Power Deliv. 24 (2) (2009) 1857–1863.

[10] S. Kamangar, H. Abyaneh, R. Chabanloo, F. Razavi, A New Genetic Algorithm Method for Optimal Coordination of Overcurrent and Earth Fault Relays in Networks with Different Levels of Voltages, in: Proceedings of the 2009 IEEE Bucharest Power Tech, Bucharest, Romania, 2011, pp. 1–5.

[11] R.M. Chabanloo, H.A. Abyaneh, S.S.H. Kamangar, F. Razavi, Optimal combined overcurrent and distance relays coordination incorporating intelligent overcurrent relays characteristic selection, IEEE Trans. Power Deliv. 26 (3) (2011) 1381–1391.

[12] M. Ezzeddine, R. Kaczmarek, A novel method for optimal coordination of directional overcurrent relays considering their available discrete settings and several operation characteristics, Electr. Power Syst. Res. 81 (2011) 1475–1481.

[13] Y. Lu, J.-L. Chung, Detecting and solving the coordination curve intersection problem of overcurrent relays in subtransmission systems with a new method, Electr. Power Syst. Res. 95 (2013) 17–27.

[14] T.R. Chelliah, R. Thangaraj, S. Allamsetty, M. Pant, Application of genetic algorithm for overcurrent relay coordination, Int. J. Electric. Power Energy Syst. 55 (2014) 341–350.

[15] J.L. Blackburn, T.J. Domin, Protective Relaying: Principles and Applications, 3rd ed., CRS Press, Boca Raton, FL, 2006.

[16] W.A. Elmore, Protective Relaying Theory and Applications, 2nd ed., CRC Press, New York, NY, 2003.

[17] J.H. Holland, Adaptation in Natural and Artificial Systems, 2nd ed., MIT Press, Cambridge, MA, USA, 1992.

[18] M. Affenzeller, S. Winkler, S. Wagner, A. Beham, Genetic Algorithms and Genetic Programming: Modern Concepts and Practical Applications, 1st ed., Chapman & Hall/CRC, Boca Raton, FL, 2009.

[19] D.E. Goldberg, Genetic Algorithms in Search, Optimization, and Machine Learning, 1st ed., Addison Wesley Professional, Boston, Mass, 1989.

[20] H. Zeineldin, E. El-Saadany, M. Salama, Optimal coordination of overcurrent relays using a modified particle swarm optimization, Electr. Power Syst. Res. 76 (11) (2006) 988–995.

[21] M.Y. Shih, A.C. Enríquez, L.M.T. Treviño, On-line coordination of directional overcurrent relays: performance evaluation among optimization algorithms, Electr. Power Syst. Res. 110 (0) (2014) 122–132.

[22] R. Christie, Power systems test case archive, IEEE 14 Bus System, Online, 2014 http://www.ee.washington.edu/research/pstca/

Carlos A. Castillo Salazar received the B.Sc. degree in Mechanical and Electrical Engineering and the M.Sc. in Electrical Power Systems from Universidad Autónoma de Nuevo León, Mexico, in 2009 and 2012, respectively. At present, he is a Ph.D. student in Electrical Engineering at the same institute.

Arturo Conde Enríquez received the B.Sc. in Mechanical and Electrical Engineering from Universidad Veracruzana, Veracruz, Mexico, in 1993, and the M.Sc. and Ph.D. degrees in Electric Engineering from Universidad Autónoma de Nuevo León, Mexico, in 1996 and 2002, respectively. Currently, he is a professor at Universidad Autónoma de Nuevo León and a member of the National Research System of Mexico.

Satu Elisa Schaeffer received the M.Sc. and D.Sc. in Computer Science and Engineering at the Helsinki University of Technology (now Aalto University) in 2000 and 2006, respectively. She is presently a professor at Universidad Autónoma de Nuevo León and a member of the National Research System of Mexico.